AJNR

Synthetic MR Imaging–Based WM Signal Suppression Identifies Neonatal Brainstem Pathways in Vivo

V.U. Schmidbauer, M.S. Yildirim, G.O. Dovjak, M. Weber, M.C. Diogo, R.-I. Milos, V. Giordano, F. Prayer, M. Stuempflen, K. Goeral, J. Buchmayer, K. Klebermass-Schrehof, A. Berger, D. Prayer and G. Kasprian

AJNR Am J Neuroradiol 2022, 43 (12) 1817-1823
doi: https://doi.org/10.3174/ajnr.A7710
http://www.ajnr.org/content/43/12/1817

Synthetic MR Imaging–Based WM Signal Suppression Identifies Neonatal Brainstem Pathways in Vivo

V.U. Schmidbauer, M.S. Yildirim, G.O. Dovjak, M. Weber, M.C. Diogo, R.-I. Milos, V. Giordano, F. Prayer, M. Stuempflen, K. Goeral, J. Buchmayer, K. Klebermass-Schrehof, A. Berger, D. Prayer, and G. Kasprian

ABSTRACT

BACKGROUND AND PURPOSE: Multidynamic multiecho sequence–based imaging enables investigators to reconstruct multiple MR imaging contrasts on the basis of a single scan. This study investigated the feasibility of synthetic MRI-based WM signal suppression (syWMSS), a synthetic inversion recovery approach in which a short TI suppresses myelin-related signals, for the identification of early myelinating brainstem pathways.

MATERIALS AND METHODS: Thirty-one cases of neonatal MR imaging, which included multidynamic multiecho data and conventionally acquired T1- and T2-weighted sequences, were analyzed. The multidynamic multiecho postprocessing software SyMRI was used to generate syWMSS data (TR/TE/TI = 3000/5/410 ms). Two raters discriminated early myelinating brainstem pathways (decussation of the superior cerebellar peduncle, medial lemniscus, central tegmental tract, and medial longitudinal fascicle [the latter 3 assessed at the level of the pons]) on syWMSS data and reference standard contrasts.

RESULTS: On the basis of syWMSS data, the decussation of the superior cerebellar peduncle (31/31); left/right medial lemniscus (31/31; 30/31); left/right central tegmental tract (19/31; 20/31); and left/right medial longitudinal fascicle (30/31) were reliably identified by both raters. On the basis of T1-weighted contrasts, the decussation of the superior cerebellar peduncle (14/31); left/right medial lemniscus (22/31; 16/31); left/right central tegmental tract (1/31); and left/right medial longitudinal fascicle (9/31; 8/31) were reliably identified by both raters. On the basis of T2-weighted contrasts, the decussation of the superior cerebellar peduncle (28/31); left/right medial lemniscus (16/31; 12/31); left/right central tegmental tract (23/31; 18/31); and left/right medial longitudinal fascicle (15/31; 14/31) were reliably identified by both raters.

CONCLUSIONS: syWMSS data provide a feasible imaging technique with which to study early myelinating brainstem pathways. MR imaging approaches that use myelin signal suppression contribute to a more sensitive assessment of myelination patterns at early stages of cerebral development.

ABBREVIATIONS: CTT = central tegmental tract; DSCP = decussation of superior cerebellar peduncle; FGATIR = fast gray matter acquisition TI inversion recovery; GA = gestational age; ICC = intraclass correlation coefficient; MDME = multidynamic multiecho; ML = medial lemniscus; MLF = medial longitudinal fascicle; syWMSS = synthetic MRI-based WM signal suppression

At early stages of brain maturation, myelination proceeds in a stepwise manner.[1] In the fetal period, myelin is first detectable in the spinal cord at about 16 weeks of gestation, followed by its developmental course cephalad along the projection tracts.[1] Thus, postnatally, the brainstem has the most myelinated tissue, while brain myelination is relatively scarce supratentorially.[1,2]

Prematurity is considered a matter of increasing interest in the medical field.[3] Because preterm birth interferes with the normal brain maturation processes, imaging modalities that enable a reliable assessment of the structural and biochemical aspects of cerebral development are greatly needed.[4-8] Currently, MR imaging is considered the diagnostic mainstay for the assessment of human brain myelination in vivo.[9,10] However, the subtle effects of small myelin quantities on conventional T1- and T2-weighted MR imaging contrasts currently limit qualitative evaluations and, therefore, impede insight into certain pathologic conditions linked to myelin delays in the neonatal period.[1]

Received July 27, 2022; accepted after revision October 14.

From the Department of Biomedical Imaging and Image-Guided Therapy (V.U.S., M.S.Y., G.O.D., M.W., R.-I.M., F.P., M.S., D.P., G.K.) and Comprehensive Center for Pediatrics (V.G., K.G., J.B., K.K.-S., A.B.), Department of Pediatrics and Adolescent Medicine, Division of Neonatology, Pediatric Intensive Care and Neuropediatrics, Medical University of Vienna, Vienna, Austria; and Department of Neuroradiology (M.C.D.), Hospital Garcia de Orta, Almada, Portugal.

Please address correspondence to Gregor Kasprian, MD, Department of Biomedical Imaging and Image-Guided Therapy, Medical University of Vienna, Waehringer Guertel 18-20, 1090 Vienna, Austria; e-mail: gregor.kasprian@meduniwien.ac.at

Indicates article with online supplemental data.

http://dx.doi.org/10.3174/ajnr.A7710

Table 1: Study sample

Neonates	$n = 31$
GA	
Born $<28 + 0$[a]	$n = 23$
Born $28 + 0$–$36 + 6$[a]	$n = 3$
Born $\geq 37 + 0$[a]	$n = 5$
Characteristics	
Female/male	13:18
GA at birth[b]	$27 + 0$ ($23 + 4$–$41 + 6$)
PMA at MR imaging[b]	$37 + 3$ ($34 + 5$–$47 + 2$)

Note:—PMA indicates postmenstrual age (ie, GA plus chronologic age[37]).
[a] Data (weeks + days) presented as total number.
[b] Data (weeks + days) presented as median and range (in parentheses).

Recent advances in synthetic imaging provide multiple contrasts (ie, TR, TE, and TI are synthetically defined in retrospect) based on the tissue-specific properties (ie, relaxation time and spin density) determined via a single multidynamic multiecho (MDME) sequence.[8,11-16] Novel inversion recovery acquisition strategies (ie, fast gray matter acquisition T1 inversion recovery [FGATIR]) use a short TI to suppress the myelin signal, therefore improving discrimination of brainstem pathways and identification of myelinated tissue.[17] While this approach has proved beneficial primarily in a neurosurgical imaging setting, there is a lack of information on the applicability of such contrasts for the assessment of neonatal brain myelination.[17-19]

This study aimed to investigate the feasibility of synthetic MRI-based WM signal suppression (syWMSS) for the qualitative evaluation of neonatal brainstem anatomy and brain myelination in vivo. Thus, 2 raters independently analyzed brainstem pathways on syWMSS data and conventionally acquired, standard-of-reference, T1- and T2-weighted MR imaging contrasts. In addition, brain myelination was assessed semiquantitatively on both imaging modalities (MDME-based versus conventionally acquired MR imaging contrasts). The results based on syWMSS data and conventionally acquired MR imaging contrasts were compared.

MATERIALS AND METHODS

Ethics Approval

The local ethics commission approved the protocol of this retrospective study. All guardians provided written, informed consent for neonatal brain MR imaging before scanning and agreed to the scientific use of the acquired imaging data.

Study Cohort

Between January 2018 and September 2020, forty-three cases of neonatal MR imaging (without detectable intracranial pathology), which included MDME data and conventionally acquired T1- and T2-weighted MR images, were collected. Neuroimaging was performed at the Department of Neuroradiology of Vienna General Hospital, Medical University of Vienna. All neonates were referred for brain MR imaging by the Department of Pediatrics and Adolescent Medicine of the same tertiary care center. Indications for MR imaging included routine imaging in former preterm infants at approximately term-equivalent ages and clinical suspicion of cerebral injury. However, only neonates in whom MR imaging ruled out pathologic abnormalities were included in this research. Studied patients (Table 1) have been reported previously. However, these studies focused on different research objectives.[8,11,15,16]

Neonatal MR Imaging, MDME Sequence, and MR Imaging Data Postprocessing

MR imaging was performed according to the institutional feed-and-wrap protocol, and infants were bedded on a vacuum mattress to reduce motion-related artifacts. All infants were imaged using a standardized neonatal MR imaging protocol (Online Supplemental Data) on an Ingenia (Philips Healthcare) 1.5T MR imaging system. The MDME sequence (axial plane, acquisition time = 5 minutes 24 seconds, TR = 3309 ms, TE = 13/100 ms, voxel = 0.9 × 1 × 4 mm, FOV = 200 × 165 × 109 mm; section number = 22, gap = 1 mm, echo-train = 10, pixel/Hz = 1.366/159.0; sense factor = 2) uses 2 repeat acquisition phases to derive information about tissue-specific relaxation time properties and proton density (phase a: application of a section-selective saturation pulse [flip angle = 120°] to saturate 1 section; and phase b: application of section-selective refocusing pulses [flip angle = 80°] and section-selective excitation pulses [flip angle = 90°] to generate a series of spin-echoes for another section).[14,20,21] The MDME data postprocessing software SyMRI (Version 11.2; SyntheticMR) was used to generate syWMSS data. Although the acquisition procedures for the original FGATIR sequences and MDME data differ, the contrast parameters to suppress myelin-related signals synthetically were applied according to the descriptions by Sudhyadhom et al[22] and Shepherd et al[17] (TR/TE/TI = 3000/5/410 ms).

Assessment of Brainstem Pathway Anatomy and Semiquantitative Evaluation of Myelination

Before evaluating MR imaging data, a critical visual review was performed by 1 neonatal imaging expert with 15 years of experience. Imaging data of inferior quality (ie, motion-degraded MR imaging acquisitions) were excluded from this investigation. In case multiple sequences were available (eg, multiple T1-weighted contrasts and so forth), those that provided the best image quality were used for further analysis. Two readers (observer 1 with 4 years of experience and observer 2 with 2 years of experience with neonatal MR imaging) independently discriminated early myelinating brainstem pathways at a given level on the basis of syWMSS data and conventionally acquired T1- and T2-weighted contrasts. Before the analysis, an evaluation was performed regarding the identifiability/ability to discriminate various brainstem tracts in terms of spatial resolution. Accordingly, the following anatomic tracts were defined for qualitative assessment: decussation of superior cerebellar peduncle (DSCP); left/right medial lemniscus (ML) (for the readers to identify separately at the level of the medulla oblongata [decussation of the ML], pons, and midbrain); left/right central tegmental tract (CTT) (for the readers to identify at the level of the pons); and left/right medial longitudinal fascicle (MLF) (for the readers to identify at the level of the pons).

Furthermore, both readers assessed myelination of the brainstem (ie, medulla oblongata, pons, and midbrain) and the posterior limb of the internal capsule semiquantitatively on syWMSS data and conventionally acquired T1- and T2-weighted contrasts using a previously described scoring system (Online Supplemental Data).[8] The allocated points for each region were totaled, resulting in a myelin total score.[8]

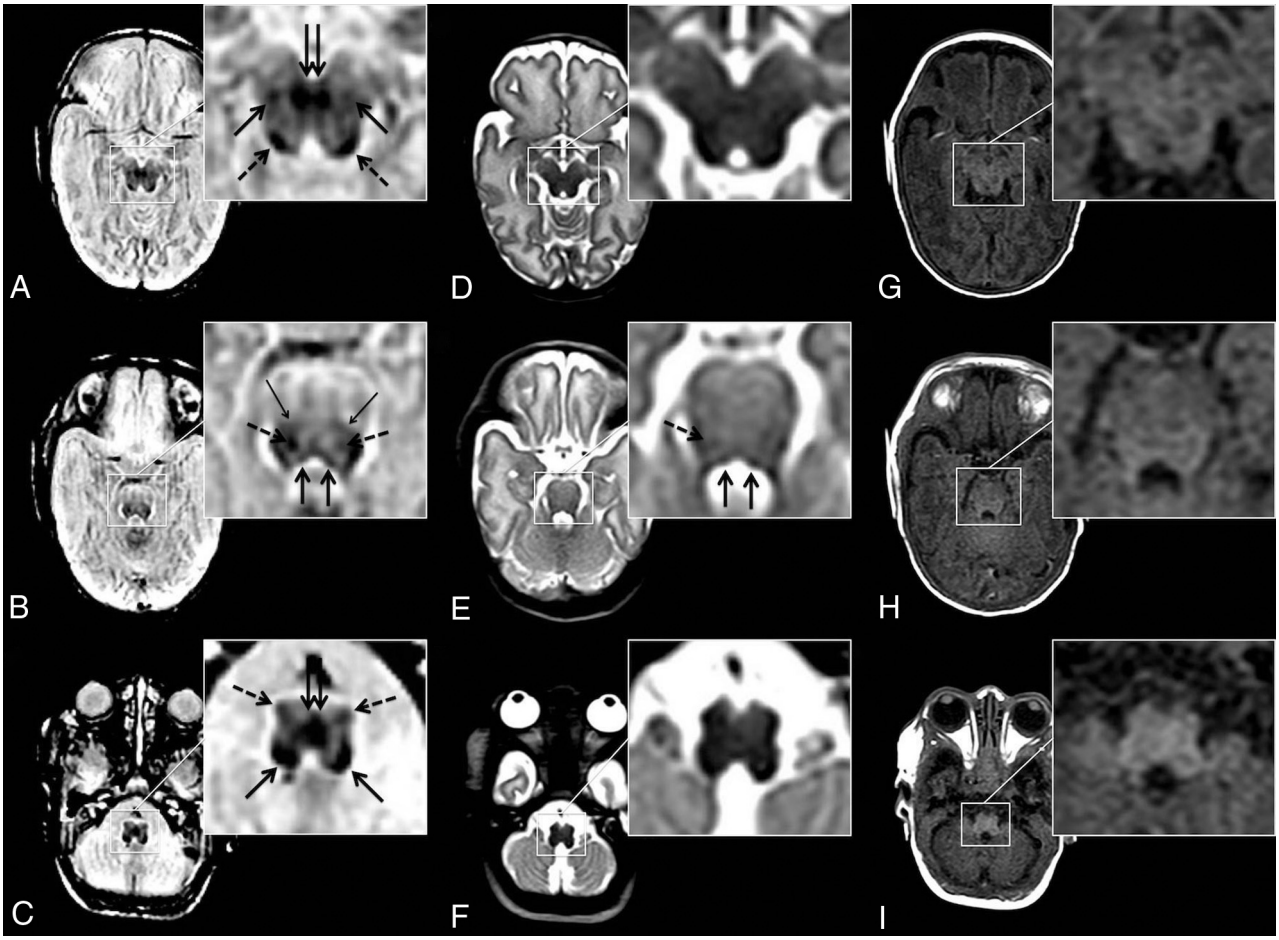

FIG 1. Neonatal brainstem anatomy is shown in an infant born at 24 + 3 weeks' GA (MR imaging at 38 + 0 weeks postmenstrual age) at the level of the midbrain (*A*, *D*, and *G*), pons (*B*, *E*, and *H*), and the medulla oblongata (*C*, *F*, and *I*) on syWMSS data (*A*, *B*, and *C*), conventional T2-weighted contrasts (*D*, *E*, and *F*), and conventional T1-weighted contrasts (*G*, *H*, and *I*). syWMSS data (*A*, *B*, and *C*) depict early myelinating structures: DSCP (*double arrow* in *A*); ML (*arrows* in *A*; *thin arrows* in *B*) and its decussation (*double arrow* in *C*); inferior colliculus (*dotted arrows* in *A*); CTT (*dotted arrows* in *B*); MLF (*arrows* in *B*); amiculum of the inferior olivary nucleus (*dotted arrows* in *C*); and inferior cerebellar peduncle (*arrows* in *C*). Pontine bundles are depicted sufficiently on T2-weighted imaging data (*D*, *E*, and *F*) (CTT [*dotted arrow* in *E*] and MLF [*arrows* in *E*]). On the basis of T1-weighted contrasts, a reliable delineation of brainstem pathways is limited (*G*, *H*, and *I*). Center/width at the reader's discretion.

A window center/width default setting was defined at 26.0/26.0 for syWMSS data. For the discrimination of brainstem pathway anatomy, the readers had the opportunity to adjust the windowing at their discretion. Semiquantitative assessment of myelination was performed at a baseline setting with a narrowed center/width range to keep myelin-related signal intensity differences perceivable and objective across the cohort.

Statistical Analysis

SPSS Statistics for Macintosh (IBM; Version 25.0) was used for statistical analyses at a significance level of $\alpha = 5\%$ ($P < .05$). All analyses were performed as proposed by 1 expert in biomedical statistics with 30 years of experience in the field. For the analysis of brainstem pathway anatomy, the percentage of interrater agreement (ie, total percentage agreement regardless of whether tracts had been correctly or not correctly identified) and the total number of tracts reliably identified by both observers (ie, only the number of tracts that had been correctly identified by both raters) were reported. To summarize overall agreement for the semiquantitative scoring (myelin total score) of neonatal brain myelination, we calculated an intraclass correlation coefficient (ICC). ICC values were interpreted as proposed by Koo and Li[23] (<0.5, poor; 0.5–0.75, moderate; 0.75–0.9, good; and >0.9, excellent). In addition, a Pearson correlation analysis was performed to detect relationships between semiquantitative myelin assessment (myelin total score) and gestational age (GA) at birth.

RESULTS

Non-motion-degraded syWMSS data were provided in 31/43 (72.09%) cases (Table 1). In 12/43 (27.91%) neonatal MDME sequence acquisitions, image quality was not sufficient for further analysis due to severe movement-related artifacts.

Assessment of Brainstem Pathway Anatomy

On the basis of syWMSS data, the percentage agreement between both raters for the discrimination of brainstem pathway anatomy ranged between 74.19% and 100% (number of tracts correctly identified by both readers; range, 18–31).

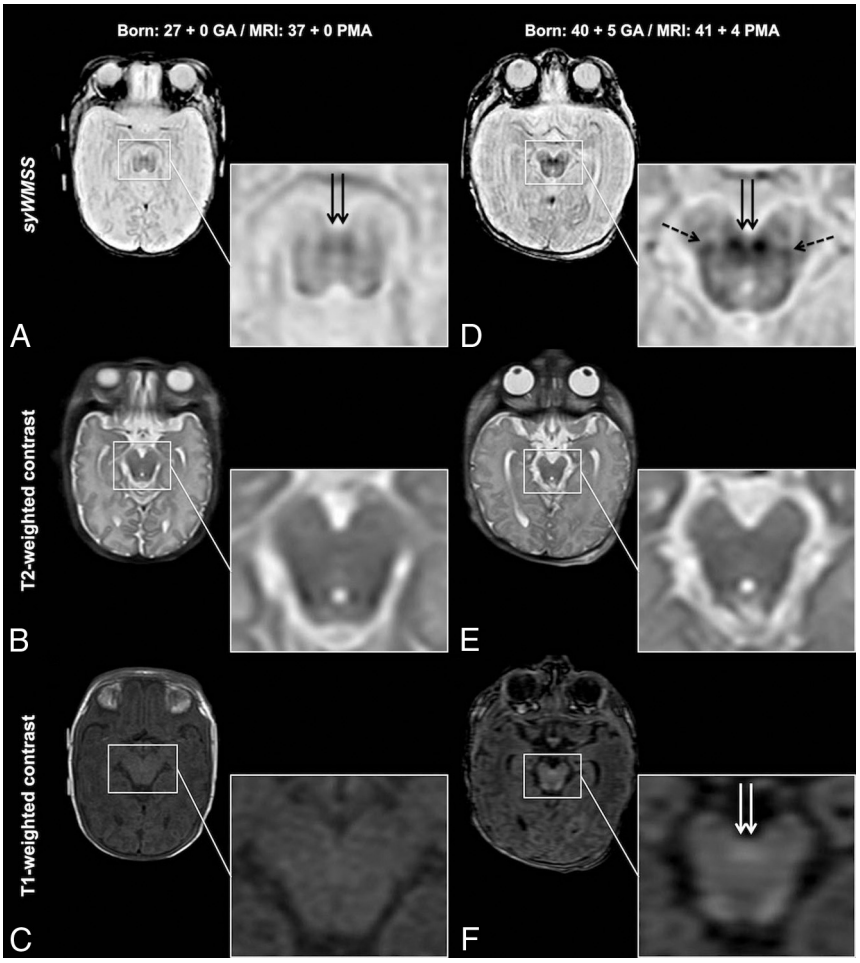

FIG 2. Myelin-related signal intensity differences between preterm-born neonates and term-born infants are demonstrated. The midbrain is shown in a neonate born at 27 + 0 weeks' GA (MR imaging at 37 + 0 weeks postmenstrual age) (*A*, *B*, and *C*) and an infant born at 40 + 5 weeks' GA (MR imaging at 41 + 4 weeks postmenstrual age) (*D*, *E*, and *F*) on syWMSS data (*A* and *D*), conventional T2-weighted contrasts (*B* and *E*), and conventional T1-weighted contrasts (*C* and *F*). While proceeding myelination is perceivable on conventional T1-weighted MR contrasts (DSCP, *double arrows* in *F*), the information provided by conventional T2-weighted MR imaging contrasts regarding myelin-related signal alterations is limited. In contrast to standard-of-reference MR imaging acquisitions, WM signal suppression enables a reliable identification and assessment of progressively myelinating structures in the course of brain development (DSCP, *double arrows* in *A* and *D* and ML, *dotted arrows* in *D*). Center/width at the default setting.

On the basis of conventionally acquired T1-weighted contrasts, the percentage agreement between both raters for the discrimination of brainstem pathway anatomy ranged between 48.39% and 80.65% (number of tracts correctly identified by both readers; range, 0–22).

On the basis of conventionally acquired T2-weighted contrasts, the percentage agreement between both raters for the discrimination of brainstem pathway anatomy ranged between 45.16% and 93.55% (number of tracts correctly identified by both readers; range, 3–28) (Fig 1 and Online Supplemental Data).

Semiquantitative Evaluation of Myelination

Significant correlations were observed between semiquantitative myelin scorings based on syWMSS data and GA at birth: $r = 0.887$ ($P < .001$) (rater 1); $r = 0.737$ ($P < .001$) (rater 2).

Significant correlations were observed between semiquantitative myelin scorings based on conventionally acquired T1-weighted contrasts and GA at birth: $r = 0.546$ ($P = .002$) (rater 1); $r = 0.495$ ($P = .005$) (rater 2).

Insignificant correlations were observed between semiquantitative myelin scorings based on conventionally acquired T2-weighted contrasts and GA at birth: $r = 0.117$ ($P = .530$) (rater 1); $r = 0.039$ ($P = .837$) (rater 2) (Figs 2 and 3).

The ICC analysis for semiquantitative myelin scoring is shown in Table 2.

DISCUSSION

In this investigation, the neonatal brainstem anatomy of early myelinating pathways was studied using synthetically generated MR imaging contrasts in which a short TI suppresses the signal of myelinated tissue.[17] Furthermore, semiquantitative assessment of myelination was performed. This study demonstrates the feasibility of syWMSS data for the identification of infratentorial WM tracts and the assessment of myelination at early developmental stages. While this novel imaging approach depicts neonatal brainstem bundles and myelinated tissue in excellent detail, conventionally acquired, standard-of-reference, T1- and T2-weighted MR imaging contrasts did not approach a similar performance.

In the second trimester, myelin becomes histologically detectable in numerous brainstem tracts.[1] While several rules govern the patterns of myelin development, the fact that tract myelination initiates according to its functionality is of note.[1] Thus, myelin deposition in neonatal brainstem pathways corresponds to essential functional circuits that ensure sensory processing and general movement at early developmental stages.[1,2] Even in the absence of gross brain damage, prematurity interferes with the regular brain-maturation processes.[24] In patients with a preterm birth history, the GA at birth correlates with the neurologic outcome, characterized by more severely impaired development in subjects born extremely prematurely (ie, <28 weeks of gestation).[6,7] Therefore, delayed myelination of brainstem pathways and disturbances in neuronal circuit integrity are associated with future neurologic deficits.[6,7,25-29] Moreover, certain pathologic conditions in the neonatal period appear directly linked to maturational delays of brainstem structures.[30-32] Evidence suggests myelination deficits and maturational delay as the potential risk factors for sudden infant death syndrome in preterm neonates.[32,33] Thus, the detection of myelin delay and the

identification of damage to these early myelinating brainstem tracts are of clinical relevance.

In this study, early myelinating brainstem pathways were more reliably identified on the basis of syWMSS data compared with the current standard-of-reference. Furthermore, assessment of brain myelination on the basis of syWMSS data revealed higher interrater agreement and stronger correlation with GA at birth than conventional MR imaging contrasts, suggesting a more reliable evaluation of cerebral development. While the potential of this sophisticated inversion recovery approach has not yet been fully investigated in pediatric cohorts, studies in the adult human brain have already revealed remarkable results. As demonstrated by Shepherd et al,[17] the suppression of myelin-related signals improves the identifiability of brainstem pathway anatomy and highly myelinated structures. Therefore, such contrasts have proved beneficial before neurosurgical interventions (eg, deep brain stimulation) because these data allow a more reliable targeting of anatomic structures.[18,19,22] The data presented here suggest that myelin signal suppression represents a feasible imaging approach for the in vivo tracking of WM pathway maturation, which is key to obtaining knowledge about normal and aberrant myelination processes throughout development.

FIG 3. Pearson correlations between GA at birth (x-axis) and myelin scorings (performed by rater 1) (y-axis) based on syWMSS data ($r = 0.887$, $P < .001$) (*A*), conventionally acquired T1WI contrasts ($r = 0.546$, $P = .002$) (*B*), and conventionally acquired T2WI contrasts ($r = 0.117$, $P = .530$) (*C*).

Table 2: ICC for semiquantitative myelin scoring[a]

	ICC
syWMSS	Moderate agreement: 0.535 (0.032–0.788)
Conventional T1-weighted	Poor agreement: 0.404 (–0.034–0.694)
Conventional T2-weighted	Poor agreement: −0.050 (−0.315–0.259)

[a] Numbers in parentheses are 95% confidence intervals.

Premature delivery accounts for approximately 7% of all births.[34] Neonatal brain MR imaging can provide biomarkers for future development.[35] However, conventional, MR imaging–based neuroimaging currently lacks sensitivity for the evaluation of delayed brain myelination.[8] The investigated imaging approach provides the opportunity to reliably characterize myelin development in vivo and may help to identify patients in need of special postnatal effort to prevent adverse future outcomes. However, this prospect was outside the scope of the present study and needs to be elucidated in future investigations.

This study has several limitations. Due to the retrospective design, the included sample size was small. In addition, most included infants were born extremely prematurely, limiting selective investigations of this imaging approach in infants born at different gestational stages. Furthermore, there was no possibility of performing a blinded data analysis. While myelin signal suppression was applied using a synthetic MR imaging–based approach, no original sequences were used to acquire imaging data in which WM-related signals are suppressed (ie, FGATIR).[17,22] Thus, the comparison of conventional and synthetic WM signal suppression was not possible. Nonetheless, as demonstrated previously, SyMRI-based imaging data provide a diagnostic accuracy comparable with that of conventionally acquired sequences.[11] However, the technical features (eg, resolution, section thickness, acquisition time, and so forth) of conventional T1- and T2-weighted imaging data and MDME sequence acquisitions differed (synthetic MR imaging–based data versus conventionally acquired sequences). Thus, partial volume effects may have increased the identifiability of certain brainstem pathways in various areas of interest, while several fibers could not be reliably identified (eg, limited identifiability of the MLF at the level of the midbrain), most likely due to resolutional issues.

Furthermore, although only MR imaging acquisitions of superior quality were included, small movement-related artifacts were still present in most of the cases. However, subject motion is still a pervasive and difficult-to-manage issue in neonatal neuroimaging. Nonetheless, overall, these limitations did not affect the primary outcome of this investigation. Finally, this study did not elaborate on the correlations between diffusion tensor–based assessments of brainstem pathway anatomy and the presented imaging approach.

However, currently, the applicability of neonatal brainstem tractography is limited, foremost due to motion-related issues.[36] Nonetheless, the relationship between advanced diffusion MR imaging fiber-tracking and MDME-based mapping is of highest interest and need to be assessed in future works.

CONCLUSIONS

Synthetically generated MR imaging contrasts with suppressed myelin-related signals provide a feasible imaging technique for the in vivo study of neonatal brainstem pathway anatomy. Furthermore, the presented MR imaging approach enables a more reliable evaluation of postnatal brain maturation compared with conventionally used, standard-of-reference, sequence-derived T1- and T2-weighted contrasts. WM signal suppression contributes to a more sensitive neuroradiologic assessment of myelination at a very early stage of cerebral development.

Disclosure forms provided by the authors are available with the full text and PDF of this article at www.ajnr.org.

REFERENCES

1. van der Knaap MS, Valk J. *Magnetic Resonance of Myelination and Myelin Disorders*. 3rd ed. Springer-Verlag; 2005
2. Yakovlev P, Lecours A. The myelogenetic cycles of regional maturation of the brain. In: Minkowski A, ed. *Regional Development of the Brain in Early Life*. Blackwell Scientific; 1967:3–70
3. Taylor GL, O'Shea TM. **Extreme prematurity: risk and resiliency.** *Curr Probl Pediatr Adolesc Health Care* 2022;52:101132 CrossRef Medline
4. Ibrahim J, Mir I, Chalak L. **Brain imaging in preterm infants <32 weeks gestation: a clinical review and algorithm for the use of cranial ultrasound and qualitative brain MRI**. *Pediatr Res* 2018;84:799–806 CrossRef Medline
5. Parikh NA. **Advanced neuroimaging and its role in predicting neurodevelopmental outcomes in very preterm infants.** *Semin Perinatol* 2016;40:530–41 CrossRef Medline
6. Glass HC, Costarino AT, Stayer SA, et al. **Outcomes for extremely premature infants.** *Anesth Analg* 2015;120:1337–51 CrossRef Medline
7. Marlow N, Wolke D, Bracewell MA, et al; EPICure Study Group. **Neurologic and developmental disability at six years of age after extremely preterm birth.** *N Engl J Med* 2005;352:9–19 CrossRef Medline
8. Schmidbauer V, Geisl G, Diogo M, et al. **SyMRI detects delayed myelination in preterm neonates.** *Eur Radiol* 2019;29:7063–72 CrossRef Medline
9. van der Knaap MS, Valk J. **MR imaging of the various stages of normal myelination during the first year of life.** *Neuroradiology* 1990;31:459–70 CrossRef Medline
10. Barkovich AJ, Kjos BO, Jackson DE, et al. **Normal maturation of the neonatal and infant brain: MR imaging at 1.5 T.** *Radiology* 1988;166:173–80 CrossRef Medline
11. Schmidbauer V, Geisl G, Cardoso Diogo M, et al. **Validity of SyMRI for assessment of the neonatal brain.** *Clin Neuroradiol* 2021;31:315–23 CrossRef Medline
12. McAllister A, Leach J, West H, et al. **Quantitative synthetic MRI in children: normative intracranial tissue segmentation values during development.** *AJNR Am J Neuroradiol* 2017;38:2364–72 CrossRef Medline
13. Tanenbaum LN, Tsiouris AJ, Johnson AN, et al. **Synthetic MRI for clinical neuroimaging: results of the magnetic resonance image compilation (MAGiC) prospective, multicenter, multireader trial.** *AJNR Am J Neuroradiol* 2017;38:1103–10 CrossRef Medline
14. Warntjes JB, Leinhard OD, West J, et al. **Rapid magnetic resonance quantification on the brain: optimization for clinical usage.** *Magn Reson Med* 2008;60:320–29 CrossRef Medline
15. Schmidbauer V, Dovjak G, Geisl G, et al. **Impact of prematurity on the tissue properties of the neonatal brainstem: a quantitative MR approach.** *AJNR Am J Neuroradiol* 2021;42:581–89 CrossRef Medline
16. Schmidbauer VU, Yildirim MS, Dovjak GO, et al. **Different from the beginning: WM maturity of female and male extremely preterm neonates: a quantitative MRI study.** *AJNR Am J Neuroradiol* 2022;43:611–19 CrossRef Medline
17. Shepherd TM, Ades-Aron B, Bruno M, et al. **Direct in vivo MRI discrimination of brainstem nuclei and pathways.** *AJNR Am J Neuroradiol* 2020;41:777–84 CrossRef Medline
18. Grewal SS, Middlebrooks EH, Kaufmann TJ, et al. **Fast gray matter acquisition T1 inversion recovery MRI to delineate the mammillothalamic tract for preoperative direct targeting of the anterior nucleus of the thalamus for deep brain stimulation in epilepsy.** *Neurosurg Focus* 2018;45:E6 CrossRef Medline
19. Bot M, Pauwels R, van den Munckhof P, et al. **The fast gray matter acquisition T1 inversion recovery sequence in deep brain stimulation: introducing the rubral wing for dentato-rubro-thalamic tract depiction and tremor control.** *Neuromodulation* 2022 Jan 15. [Epub ahead of print] CrossRef Medline
20. Hagiwara A, Warntjes M, Hori M, et al. **SyMRI of the brain: rapid quantification of relaxation rates and proton density, with synthetic MRI, automatic brain segmentation, and myelin measurement.** *Invest Radiology* 2017;52:647–57 CrossRef Medline
21. Kang KM, Choi SH, Kim H, et al. **The effect of varying slice thickness and interslice gap on T1 and T2 measured with the multidynamic multiecho sequence.** *Magn Reson Med Sci* 2019;18:126–33 CrossRef Medline
22. Sudhyadhom A, Haq IU, Foote KD, et al. **A high resolution and high contrast MRI for differentiation of subcortical structures for DBS targeting: the fast gray matter acquisition T1 inversion recovery (FGATIR).** *Neuroimage* 2009;47:T44–52 CrossRef Medline
23. Koo TK, Li MY. **A guideline of selecting and reporting intraclass correlation coefficients for reliability research.** *J Chiropr Med* 2016;15:155–63 CrossRef Medline
24. Provenzi L, Scotto di Minico G, Giorda R, et al. **Telomere length in preterm infants: a promising biomarker of early adversity and care in the neonatal intensive care unit?** *Front Endocrinol (Lausanne)* 2017;8:295 CrossRef
25. Dieterich M, Brandt T. **The bilateral central vestibular system: its pathways, functions, and disorders.** *Ann N Y Acad Sci* 2015;1343:10–26 CrossRef Medline
26. Eshaghi Z, Jafari Z, Jalaie S. **Static balance function in children with a history of preterm birth.** *Med J Islam Repub Iran* 2015;29:310 Medline
27. Kuczynski AM, Carlson HL, Lebel C, et al. **Sensory tractography and robot-quantified proprioception in hemiparetic children with perinatal stroke: sensory tractography in perinatal stroke.** *Hum Brain Mapp* 2017;38:2424–40 CrossRef Medline
28. Günal A, Pekçetin S, Öksüz Ç. **Sensory processing patterns of young adults with preterm birth history.** *Somatosens Mot Res* 2020;37:288–92 CrossRef Medline
29. Kwong AK, Doyle LW, Olsen JE, et al. **Early motor repertoire and neurodevelopment at 2 years in infants born extremely preterm or extremely-low-birthweight.** *Dev Med Child Neurol* 2022;64;855–62 CrossRef Medline
30. Jost K, Pramana I, Delgado-Eckert E, et al. **Dynamics and complexity of body temperature in preterm infants nursed in incubators.** *PLoS One* 2017;12:e0176670 CrossRef Medline
31. Knobel RB, Levy J, Katz L, et al. **A pilot study to examine maturation of body temperature control in preterm infants.** *J Obstet Gynecol Neonatal Nurs* 2013;42:562–74 CrossRef Medline
32. Sarnat HB, Flores-Sarnat L, Auer RN. **Sequence of synaptogenesis in the fetal and neonatal cerebellar system, Part 1: Guillain-Mollaret triangle (dentato-rubro-olivo-cerebellar circuit).** *Dev Neurosci* 2013;35:69–81 CrossRef Medline
33. Kinney HC, Brody BA, Finkelstein DM, et al. **Delayed central nervous system myelination in the sudden infant death syndrome.** *J Neuropathol Exp Neurol* 1991;50:29–48 CrossRef Medline

34. Kramarz S. **Preterm birth rate in Germany: no numbers exist for this.** *Dtsch Arztebl Int* 2020;117:509 CrossRef Medline
35. Goeral K, Kasprian G, Hüning BM, et al. **A novel magnetic resonance imaging-based scoring system to predict outcome in neonates born preterm with intraventricular haemorrhage.** *Dev Med Child Neurol* 2022;64:608–77 CrossRef Medline
36. Dubois J, Alison M, Counsell SJ, et al. **MRI of the neonatal brain: a review of methodological challenges and neuroscientific advances.** *J Magn Reson Imaging* 2021;53:1318–43 CrossRef Medline
37. Engle WA, American Academy of Pediatrics Committee on Fetus and Newborn. **Age terminology during the perinatal period.** *Pediatrics* 2004;114:1362–64 CrossRef Medline